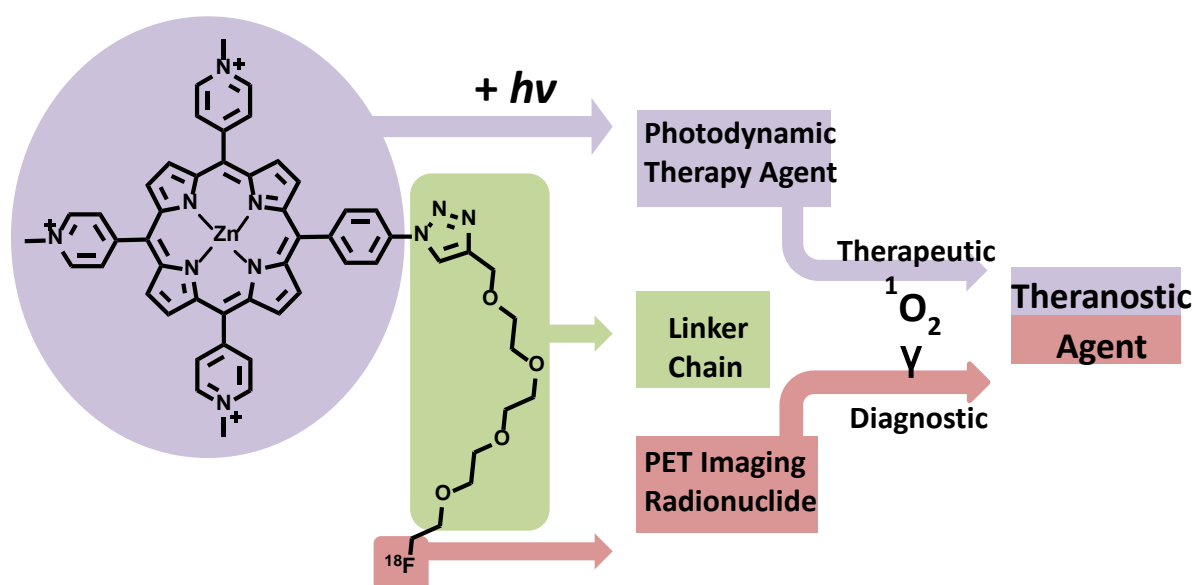


Development of PDT/PET Theranostics: Synthesis and Biological Evaluation of a ^{18}F - Radiolabeled Water Soluble Porphyrin

Guy M. Entract¹, Francesca Bryden^{1,2}, *Juozas Domarkas^{1,2}*, Huguette Savoie¹, Louis Allott³,
Stephen J. Archibald^{1,2}, *Chris Cawthorne^{2,4}*, Ross W. Boyle^{*1}

1. Department of Chemistry, University of Hull, Cottingham Road, Hull, Yorkshire HU6 7RX, UK 2. Positron Emission Tomography Research Centre, University of Hull, Cottingham Road, Hull, HU6 7RX, UK 3. Institute of Cancer Research, 123 Old Brompton Road, London, SW7 3RP, UK 4. School of Biological, Biomedical and Environmental Sciences, University of Hull, Cottingham Road, Hull, Yorkshire, HU6 7RX, UK.



Abstract

Synthesis of the first water-soluble porphyrin radiolabeled with fluorine-18 is described; a new molecular theranostic agent which integrates the therapeutic selectivity of photodynamic therapy (PDT) with the imaging efficacy of positron emission tomography (PET). Generation of the theranostic was carried out through the conjugation of a cationic water-soluble porphyrin bearing an azide functionality to a fluorine-18 radiolabeled prosthetic bearing an alkyne functionality through click conjugation, with excellent yields obtained in both cold and hot synthesis. Biological evaluation of the synthesised structures shows both the first example of an ^{18}F -radiolabeled porphyrin retaining photocytotoxicity following radiolabeling, as well as demonstrable conjugate uptake and potential application as a radiotracer *in vivo*. The promising results gained from biological evaluation demonstrate the potential of this structure as a clinically-relevant theranostic agent, offering exciting possibilities for the simultaneous imaging and photodynamic treatment of tumours.

Keywords

Fluorine-18, PET imaging, Photodynamic Therapy, Porphyrins, Theranostics

Introduction

A growing interest in the development of theranostics and “personalised medicine” highlights the utility of dual-functional theranostic compounds, which combine diagnostic and therapeutic modalities within the same agent, for the treatment of neoplastic conditions. Therapeutic strategies exploited to date include nucleic acid delivery, chemotherapy, hyperthermia (photo-thermal ablation), photodynamic therapy, and radiation therapy, coupled with imaging strategies including MRI, fluorescent markers, single-photon emission computed tomography (SPECT), and positron emission tomography (PET).¹

Porphyrins offer excellent potential as theranostic agents for personalised medicine; their potent cytotoxic activity within the field of photodynamic therapy has been well documented,² demonstrating their increasing clinical relevance in these treatment modalities.³⁻⁵ In addition, porphyrins demonstrate potential as imaging agents from the inherent fluorescence of the tetrapyrrolic core, and also their ability to chelate metals suitable for PET, SPECT and MRI (see Boyle *et al.*² for a comprehensive review). PET in particular offers quantitative imaging of physiological and pathophysiological activities *in vivo* and is well-suited for oncology and whole body imaging.⁶

Some progress has been made towards functionalising PDT agents with positron-emitting radionuclides for use in PET; however, to date the vast majority of radiolabeling strategies have utilised porphyrins as chelating agents for radioisotopes such as ⁶⁴Cu, ^{68/67}Ga, ¹⁴⁰Nd and ¹⁶⁶Ho⁷⁻¹² (see Waghorn *et al.*¹³ for a comprehensive review of radiolabeled porphyrins). Unfortunately, this strategy can inhibit the therapeutic potential of the porphyrin photosensitiser, as chelation of paramagnetic isotopes quench the photocytotoxic action of the porphyrin, rendering it useless as a therapeutic agent. These limitations encouraged us to investigate the attachment of non-metal positron emitting radionuclides onto photodynamically active porphyrins.

Fluorine-18 is often referred to as the “radionuclide of choice” for PET imaging agents. The 109.8 minute half-life permits the use of multistep synthesis and allows ample time for transportation to the clinic, whilst the high proportion of positron decay and relatively low energy of emitted positrons/positron range facilitate high resolution PET imaging. Despite this, examples of porphyrins and other tetrapyrrolic photosensitisers radiolabeled with fluorine-18 in the literature are limited. While methods for fluorine-18 radiolabeling of a porphyrin¹⁴ and a phthalocyanine¹⁵ have been described, neither of these methods are ideal; both require extended reaction times and harsh reaction conditions, with radiochemical yields of less than

25% achieved. In addition, neither demonstrated retention of the cytotoxic action of the photosensitiser following radiolabeling.

Following our current interest in porphyrin bioconjugation using the Copper (I) –Catalysed Alkyne-Azide Cycloaddition (CuAAC) reaction¹⁶⁻¹⁸, it was rationalised that a click conjugation methodology could be utilised to radiolabel a porphyrin under mild reaction conditions, providing a mild and high yielding method for radiolabeling water-soluble porphyrins with minimal impurities.¹⁹

Results and Discussion

The requirement that we considered essential for designing a porphyrin-fluorine-18 labeled theranostic agent was that it should combine the activity of both a radiotracer and a photocytotoxic therapeutic agent. Additionally, the half-life of the chosen radionuclide dictated that the synthesis be quick and facile, while offering a simple but efficient purification. The agent was required to be water-soluble, to allow administration without complex formulation. To date, there have been no reports of fluorine-18 labeled porphyrins exhibiting these requirements.

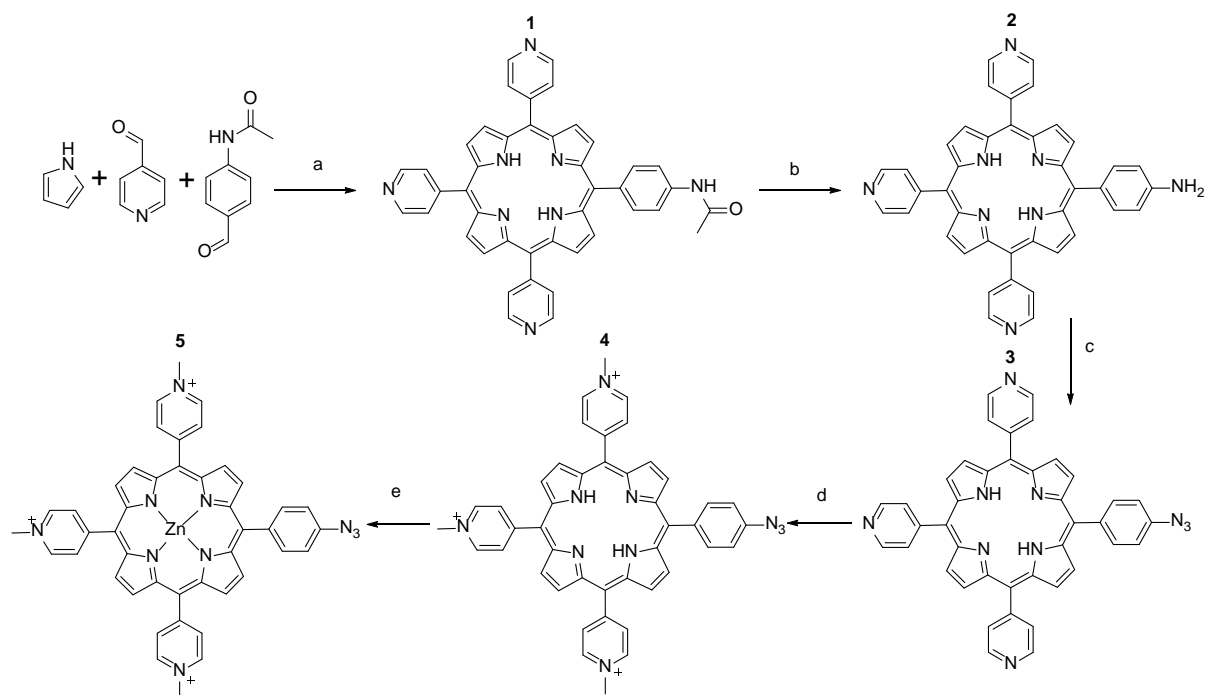
Our synthetic route (Scheme 1) utilized a water-soluble cationic porphyrin bearing an azide clickable moiety, and a PEG chain bearing an alkyne clickable moiety. The fluorine labeled PEG chain was then clicked to the porphyrin by CuAAC reaction to afford the product.

Porphyrin Synthesis and Characterization

Porphyrin **2** was obtained from the hydrolysis of porphyrin **1** according to a previously published procedure²⁰ in 75 % yield. Subsequent synthesis of porphyrin **3**¹⁷ was accomplished

by diazotization of the amine precursor, with **3** obtained in a yield of 97 %. Methylation to produce porphyrin **4** was carried out with methyl iodide to produce the water-soluble, cationic pyridiniumyl porphyrin **4**²¹ giving a 90 % yield, with ammonium hexafluorophosphate/tetrabutylammonium chloride workup carried out to facilitate anion substitution and product purification.¹⁸

At this stage, zinc chelation of the porphyrin was required to prevent complexation of the copper catalyst used in the click reaction by the free base porphyrin. While chelation of the paramagnetic copper catalyst can both interfere with the CuAAC reaction, and quench any PDT effect of the porphyrin, similar zinc chelated porphyrins have been shown to resist copper metallation and also demonstrate potent photocytotoxicity²².

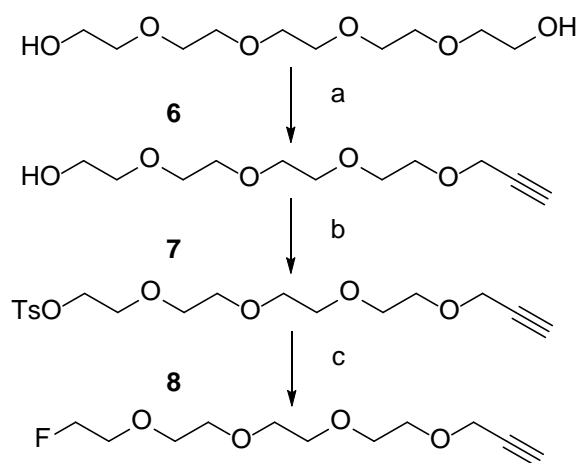


Scheme 1. (a) propionic acid, 180 °C 1 hr, (b) 12 M HCl 100 °C 3 hr, then DCM/TEA 9:1 10 min, (c) NaNO₂ soln. and TFA at 0 °C 15 min, then NaN₃ soln. added 0 °C 1 hr (d) CH₃I in

DCM 40 °C 18h, counter-ion exchange NH_4PF_6 and TBAC, (e) $\text{Zn}(\text{OAc})_2$ in water rt 30 mins, then counter-ion exchange NH_4PF_6 and TBAC.

Functionalized PEG Chain Synthesis and Characterization

Two examples of heterobifunctional tetraethylene glycol chains were synthesized to act as carriers for ^{18}F , both functionalized with alkyne groups to allow facile click conjugation to the photosensitiser. The tetraethoxy PEG chain was selected as a synthetic target due to the low volatility and excellent amphiphilicity of this structure making it an ideal target for safe and biocompatible radiolabeling. While **7** was produced with a tosyl group for radiolabeling *via* substitution with fluorine-18, fluorine-functionalized **8** was utilized both for radiolabeling *via* isotopic substitution and for cold cytotoxicity studies.



Scheme 2. (a) NaH in THF at -20 °C. Propargyl bromide at rt 18h under N_2 , (b) TsCl, TEA, DCM. N_2 rt 17 h, (c) anhydrous THF under argon, 80 °C, 1 M TBAF in THF.

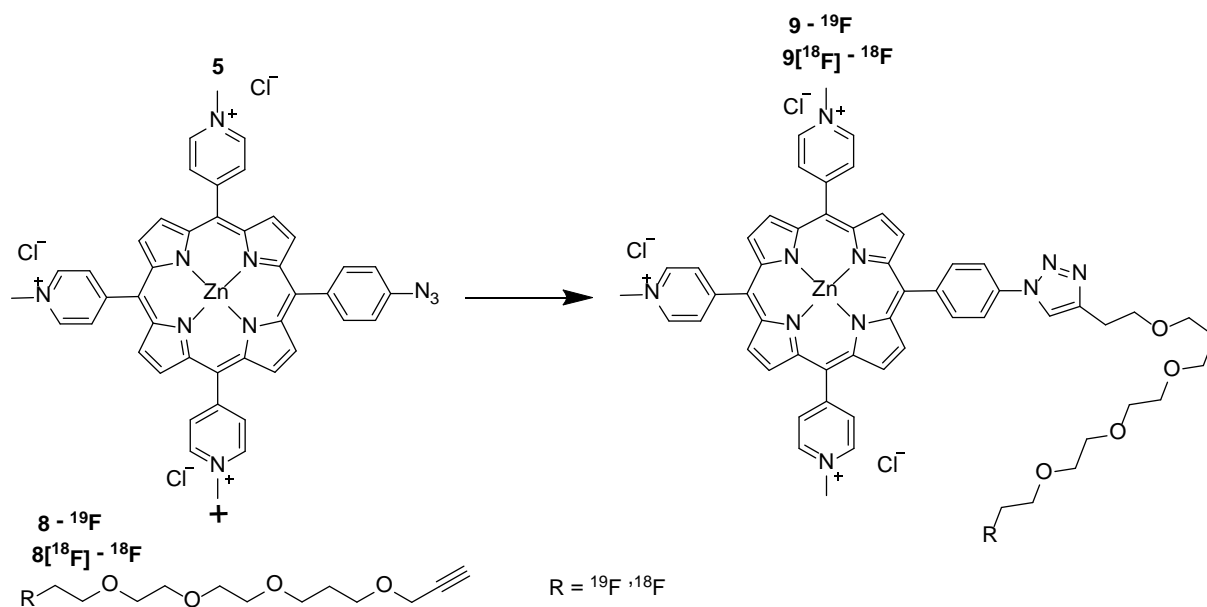
Synthesis of **6** from (OH-PEG₅-OH) was carried out according to a literature procedure²³ to yield 68 % as a pale yellow oil. Tosylation was then carried out²⁴ to produce **7** in 80 % yield. The synthesis of **8** was initially performed using ^{19}F in the form of TBAF, with TLC monitoring

showing almost instantaneous generation of **8** from **7** in 90% yield, with product identity confirmed by NMR and MS.

Click Conjugation of Porphyrin and Functionalized PEG Chain

To afford synthetic flexibility, initially, click conjugation of **7** and **8** to porphyrin **5** was attempted, with the aim of producing a porphyrin which could undergo radiolabeling in a one-step process. However, this direct labelling methodology was found to be unsuitable for two reasons; in the presence of a source of fluoride ions porphyrin **5** was found to undergo counter ion exchange on the pyridiniumyl cationic moieties, producing a product with poor water-solubility and labile fluoride which could easily dissociate *in vivo*. Secondly, it was found that under the described conditions, the tosylated PEG chain did not undergo the click reaction. As a result, click conjugation was then carried out utilising chain **8** only, allowing both cold optimisation of the click methodology, as well as production of a cold standard of porphyrin conjugate **9** for both analysis and biological evaluation (Scheme 3).

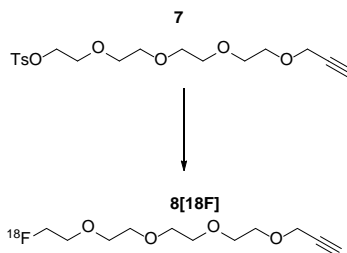
Conjugate **9** was synthesized by CuAAC reaction. In contrast to the tosylated chain **7**, **8** was found to undergo rapid and high-yielding click conjugation under the described conditions, affording the product **9** in excellent yield (90%). Reaction progress was monitored by both TLC and HPLC; the developed HPLC methodology also provided good separation between the precursors and final product, allowing for semi-preparative HPLC purification to isolate the radiolabeled product.



Scheme 3. Copper (II) sulfate, sodium ascorbate and TBTA in 1:3 THF: MW 40 °C, 60W, 15 min.

^{18}F labelling of PEG Chain

Generation of the radiolabeled prosthetic group $8[^{18}\text{F}]$ was achieved *via* (Scheme 4 nucleophilic substitution of the tosyl group. Initially, reaction of dried fluorine-18 with chain **8** was investigated.



Scheme 4. (a) dried ^{18}F , 140 °C, 10 min. (b) dried ^{18}F , 180 °C, 10 min.

8 was heated with dry ^{18}F at $180\text{ }^\circ\text{C}$ for 10 minutes, giving an expected low incorporation of $4.48\% \pm 1.37$ ($n = 3$) ^{18}F (Figure 1), with increased heating times showing no significant variation. Nucleophilic substitution of **7** demonstrated excellent ^{18}F labelling, with heating for 10 minutes at $140\text{ }^\circ\text{C}$ resulting in a $93.4\% \pm 3.34$ ($n = 3$) radiochemical yield (Figure 2).

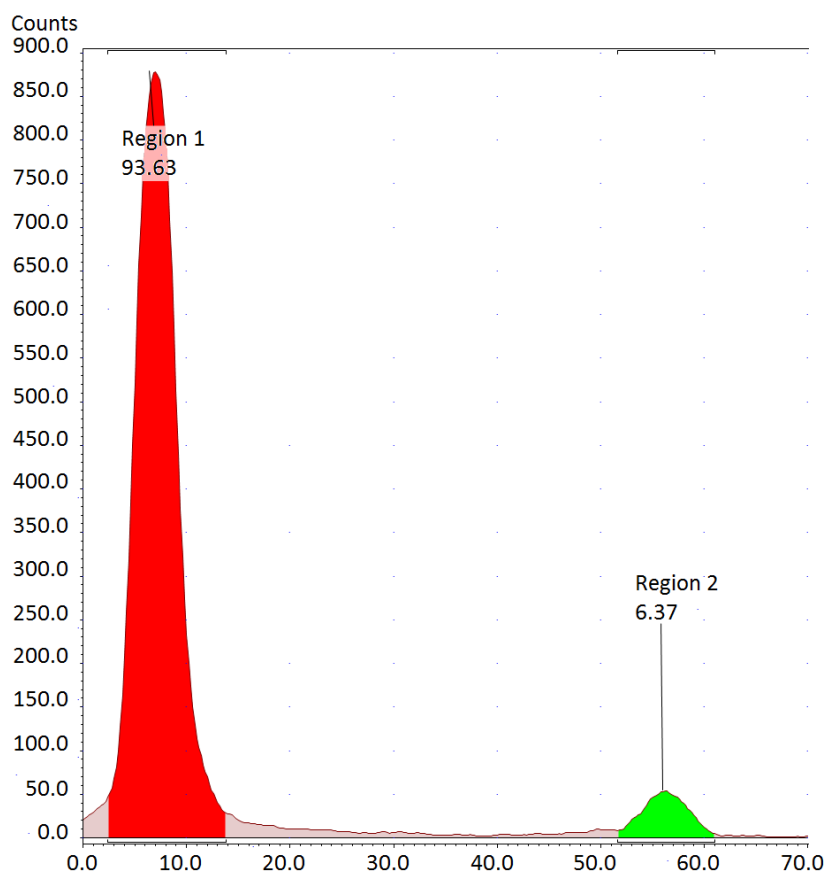


Figure 1. RadioTLC of the isotopic substitution reaction, showing $<5\%$ incorporation. Region 1: free ^{18}F , Region 2: incorporated ^{18}F

Purification of **8** from the precursor **7** was carried out on Sep-Pak®Light tC18 cartridges, to remove residual free ^{18}F , with the product obtained in $>99\%$ radiochemical purity. Alternatively, generation of the a carrier-added derivative was found to be possible, with residual **7** reacted with

TBAF to produce a $^{19}\text{F}/^{18}\text{F}$ mixture, giving a single chemical product with no reduction in ^{18}F incorporation observed.

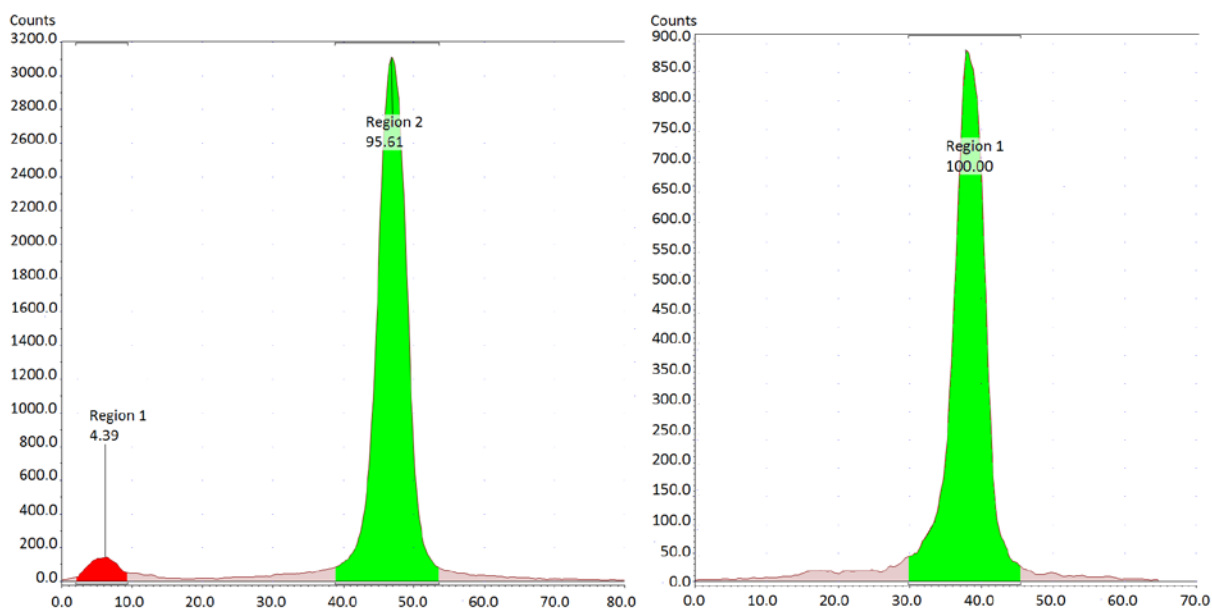


Figure 2. RadioTLC of the substitution reaction, showing >95% incorporation (left) and >99% radiochemical purity following purification (right).

Radiolabeled porphyrin conjugate synthesis and characterisation

As previously discussed, under click conditions chain **8** demonstrates excellent conjugation yields with porphyrin **5**, while the precursor **7** shows no reaction with the same porphyrin. Conveniently, click reaction of mixtures of both **7** and **8** with porphyrin **5** were also found to yield porphyrin **9** exclusively, and therefore no HPLC purification of the mixture was required.

CuAAC reaction of the photosensitiser **5** with the radiolabeled chain **8**[^{18}F] was performed by heating at 40 °C for 20 minutes under previously described conditions. The mixture was purified on a Sep-Pak® Light tC18 cartridge and washed several times with water before the product was eluted with ethanol. Incorporation yields of final product **9**[^{18}F] were 34.2 % \pm 2.46 (n = 3) (Figure 3).

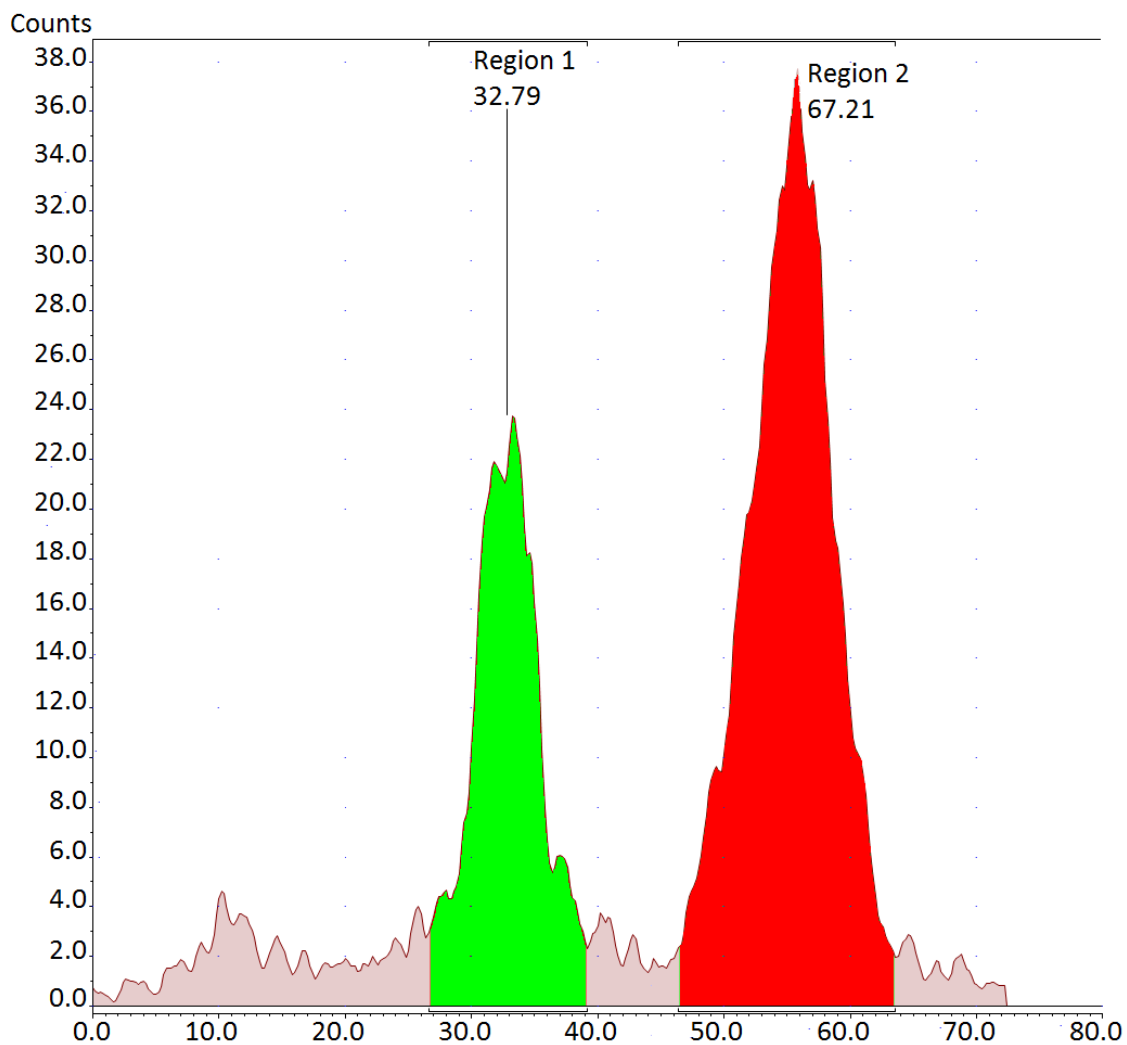


Figure 3. RadioTLC of click reaction; 32.8% incorporation of fluorine-18 within **9**[¹⁸F] (Region 1).

Evaluation of cytotoxicity

Confirmation of the potential of conjugate **9** as a therapeutic agent was carried out through the evaluation of the photocytotoxicity of the conjugate in a human adenocarcinoma (HT-29) cell line. Irradiation of **9** was carried out using an Oriel light system filtered to remove light below 550 nm,

and the results were compared to a non-irradiated control. The irradiated light chosen aligns well with the two Q-bands of the zinc chelated porphyrin, while excluding the Soret band, giving results which would be applicable to both *in vivo* testing and clinical use. Human colon adenocarcinoma cells (HT-29) were incubated for 1 hr with increasing concentrations of **9**, and irradiated with light (> 550 nm) giving an LD₉₀ of approximately 1×10^{-4} M (Figure 4), with minimal dark toxicity (>75 % cell survival), observed for all non-irradiated conditions.

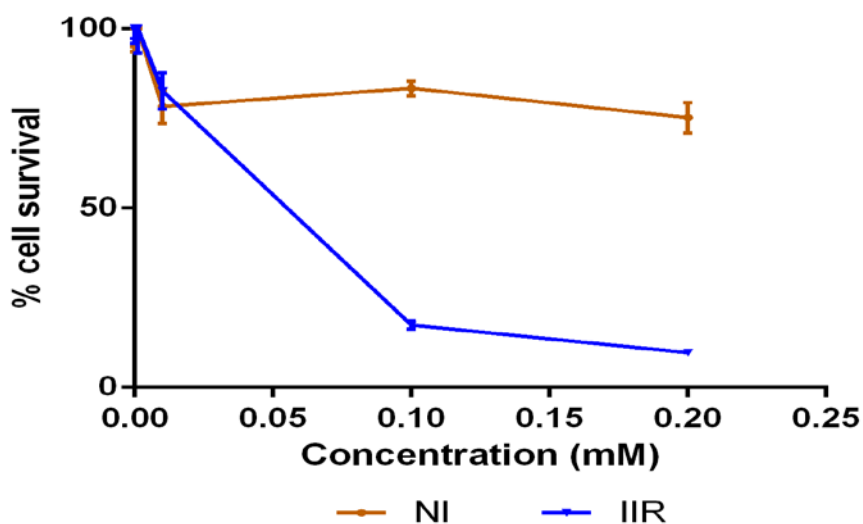


Figure 4. Graph of cytotoxicity assay. Assay was carried out on HT-29 cell lines, with results displayed for conjugate **9** following irradiation (IRR) and non-irradiated control (NI).

Fluorescence and bright field images (Figure 5) of photosensitizer accumulation in the HT-29 cell line were also acquired, demonstrating cellular uptake of the photosensitizer in this cell line. The bright field image also exhibits blebbing around the cell membrane, indicating rapid onset apoptosis due to photosensitizer activation by the excitation source of the microscope, behaviour which has previously been reported for cationic porphyrins.²⁵

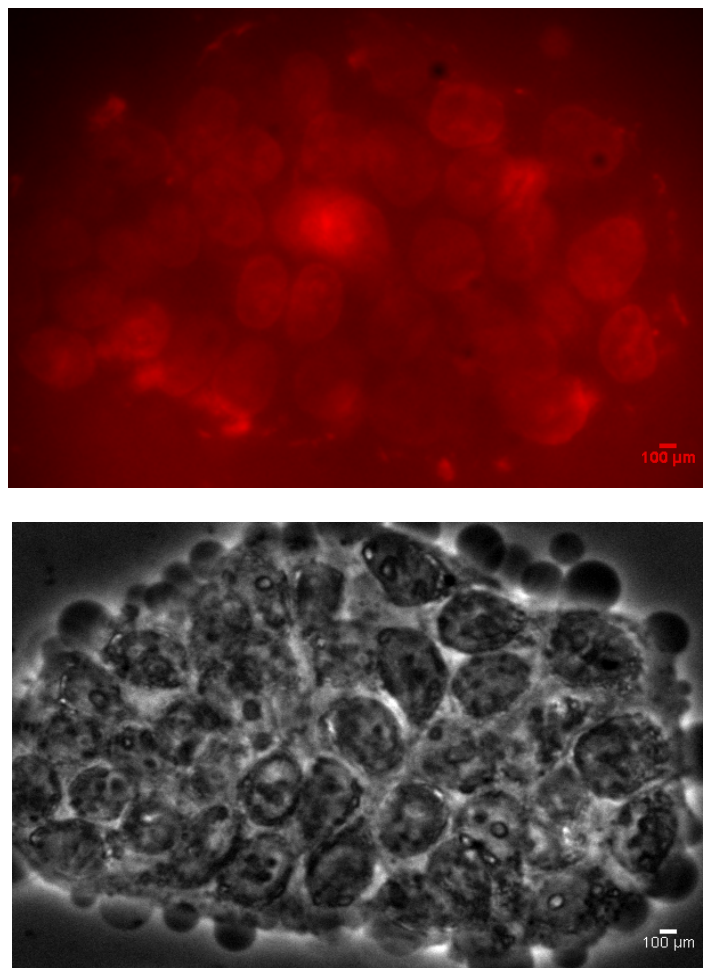


Figure 5. (Top Image) Fluorescence image showing cellular uptake of photosensitizer **9** in human adenocarcinoma (HT-29) cells, (Bottom Image) Bright field image of HT-29 cells incubated with **9**.

***In vivo* radiochemistry**

Preparation of the **8**[¹⁸F] and subsequent click reaction to form conjugate **9**[¹⁸F] was performed as described in the experimental, with both crude **8**[¹⁸F] and **9**[¹⁸F] purified by semi-preparative HPLC after each stage of the reaction. Fluorination of **8**[¹⁸F] was carried out in acetonitrile, to yield the product in 77 % RCY (non-decay corrected) and >99% RCP by HPLC. Click reaction to

the porphyrin was then carried out at 60°C to produce **9**[¹⁸F] in 16 % RCY (non-decay corrected) and >97 % RCP by HPLC. The isolated sample of **9**[¹⁸F] demonstrated good specific activity of 1GBq/μmol, with an obtained *log P* value of -2.48 (PBS:octanol).

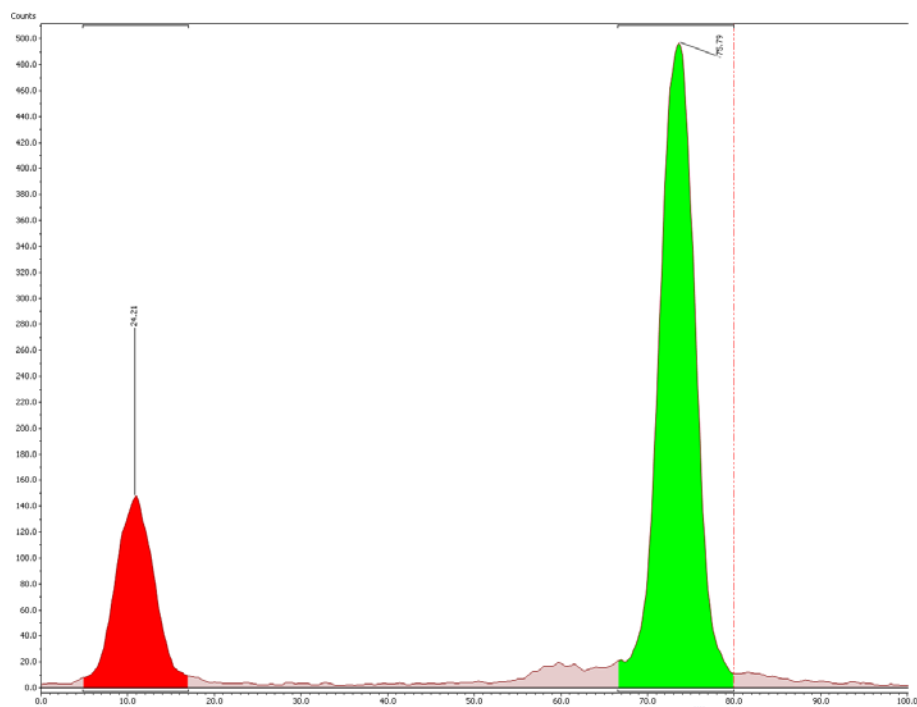


Figure 6 . RadioTLC of the nucleophilic substitution synthesis of **8**[¹⁸F], showing >75 % incorporation.

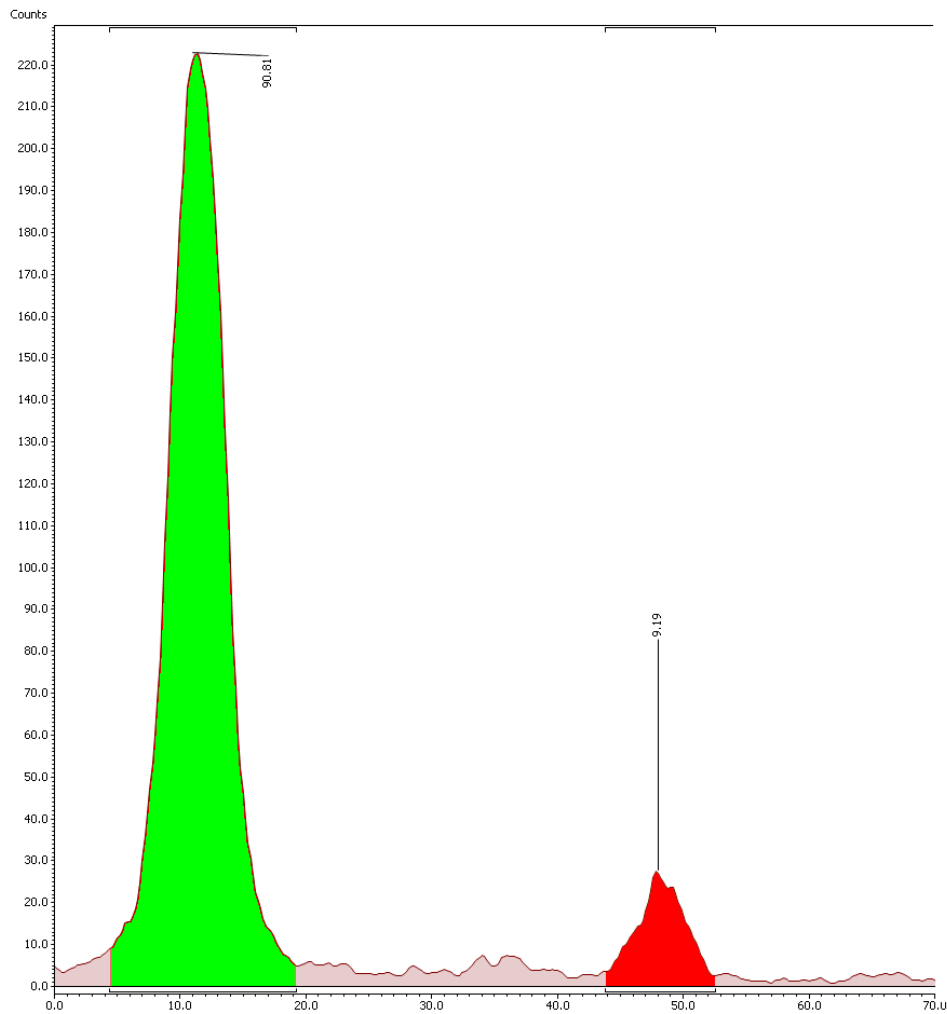


Figure 7. RadioTLC of click reaction synthesis of **9**[¹⁸F], with over 66% incorporation demonstrated.

***In vivo* evaluation**

Tumour uptake was assessed in the HT29 and U87 xenograft models. Conjugate **9**[¹⁸F] was injected intravenously (i.v.) and biodistribution was quantified by PET imaging (8).

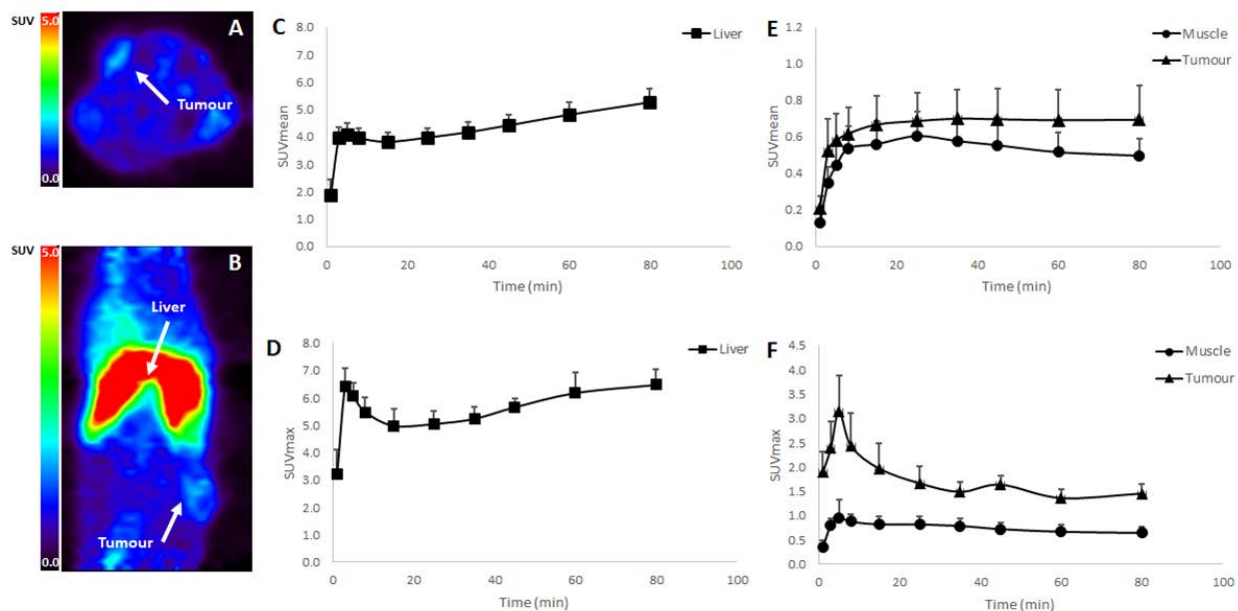


Figure 8. Dynamic $^9\text{[}^{18}\text{F]}$ uptake in tumour bearing animals. A and B: Transaxial and coronal image slices centred on the tumour at 80-90 minutes, showing uptake in tumour and liver in representative HT29 tumour (arrows). C, D: Time activity curves of $^9\text{[}^{18}\text{F]}$ in liver E,F: Time activity curves of $^9\text{[}^{18}\text{F]}$ in tumour and muscle. All time activity curves represent average data from four tumour-bearing animals \pm S.E.M.

As expected, $^9\text{[}^{18}\text{F]}$ accumulated mainly in the liver (Figure 8 C&D), consistent with previously reported data on porphyrins¹³. There was also evidence of tumour accumulation in both models, with average tumour-to-muscle ratios of 1.4 (SUVmean) or 2.3 (SUVmax) at 80-90 minutes (Figure 8 E&F). The accumulation of untargeted porphyrins in tumour tissue is thought to be due to the enhanced permeability and retention (EPR) effect, and this is assumed to be high in preclinical xenograft models²⁶. For the purposes of this study we assessed uptake in HT29 and U87 tumours, as these have been reported to effect low or high levels of EPR mediated

nanoparticle accumulation respectively^{27,28}. Tumour uptake was observed in all tumours, exhibiting the potential of this theranostic agent for calculating the optimal irradiation time for clinical PDT treatment.

Conclusions

In conclusion, we have demonstrated that a single theranostic agent in the form of a novel fluorine-18 radiolabeled water-soluble porphyrin can be synthesized from an alkyne-bearing ¹⁸F PEG carrier chain and an azide functionalised porphyrin. This is the first demonstration of an ¹⁸F radiolabeled porphyrin retaining photocytotoxicity following radiolabeling; with the synthesised compound showing cellular uptake, good photocytotoxicity and minimal dark toxicity in a relevant human cancer cell line, as well as confirmed uptake of the conjugate into neoplastic tissue and demonstrated potential as a radiotracer *in vivo*. The promising results gained from biological evaluation demonstrate the potential of this structure as a clinically-relevant theranostic agent, offering exciting possibilities for the simultaneous imaging and photodynamic treatment of tumours.

Experimental

Materials and methods

¹H and ¹³C NMR spectra were recorded on JEOL Eclipse 400 and JEOL Lambda 400 spectrometers (operating at 400 MHz for ¹H and 100 MHz for ¹³C). Chemical shifts (δ) are reported in parts per million (ppm), referenced to CDCl₃ and DMSO. Coupling constants (J) are recorded in Hz and significant multiplicities described by singlet (s), doublet (d), multiplet (m). MALDI mass spectra were performed by the EPSRC National Mass Spectrometry Facilities, Swansea, UK. UV-visible spectra were recorded on a Varian Cary spectrophotometer. Chemical reagents and

solvents were purchased from Sigma-Aldrich and Alfa Aesar, and were used as received unless otherwise stated. Microwave reactions were carried out in a CEM Discover Benchmate microwave reactor controlled using Synergy software. In all cases, maximum stirring, maximum pressure of 200 bar and 2 minute maximum heating step were used. Reaction temperatures were monitored using an external IR probe and carried out in a 10 ml sealed reaction vessel. Irradiation of cells during phototoxicity assays was carried out using an Oriel lamp system with a Schott 06515 Long Pass Optical Filter, allowing irradiation with 95–98% of light above 515 nm. Fluorine-18 (^{18}F) was produced by the $^{18}\text{O}(\text{p}, \text{n})^{18}\text{F}$ nuclear reaction using a 7.5 MeV ABT Biomarker Generator cyclotron (ABT Molecular Imaging, Inc.©, USA) and [^{18}O]H₂O >98% (CMR©, Russia), being the current reaching the target ~4.2 μA . Specific activity of the produced ^{18}F was an average of 100 GBq.mol⁻¹, according to the manufacturer. Analytical HPLC was performed through an Agilent 1200 series with a 254 nm UV detector (Agilent Technologies©, USA) and effluent radioactivity was monitored using a NaI crystal coupled to a photomultiplier tube (LabLogic Systems Limited©, UK). Purification by semi-preparative HPLC was performed through an Agilent 1100 series with a 254 nm UV detector (Agilent Technologies©, USA) and effluent radioactivity was monitored using a NaI crystal coupled to a photomultiplier tube (LabLogic Systems Limited©, UK). An ACE 5 C18 10*250 5A column was used, with all products eluted using MeCN:water gradients containing 0.1% TFA (flow rate 4.7 ml/min).

Synthetic procedures

Synthesis of **4**: Methyl iodide (2 ml, 32.3 mmol) was added via syringe to a stirred solution of 5-[4- azidophenyl]-10,15,20-tri-(4-pyridyl) porphyrin (100 mg, 0.151 mmol) in dimethyl formamide (DMF) (10 ml). The reaction was then stirred at 40 °C overnight. After filtering through

cotton wool, the residue was dissolved in water. Ammonium hexafluorophosphate was added, and the product filtered. The solid was dissolved in acetone and tetrabutylammonium chloride was added, and the mixture filtered. The crude product was precipitated from diethyl ether over MeOH to yield a dark brown solid (148 mg, 90%). UV-vis (H₂O): max, 424, 520, 562, 590, 648. log (424 nm) = 5.11 M⁻¹cm⁻¹. ¹H-NMR (DMSO-d₆): δ 4.74 (s, 9H, CH₃), 7.65 (d, 2H, 5-m-Ph), 8.28 (d, 2H, 5-o-Ph), 9.01 (m, 6H, 10,15,20-o-Py), 9.12 (m, 8H, βH), 9.07 (m, 6H, 10,15,20-m-Py). ¹³C-NMR (DMSO-d₆): δ 40.13 (CH₃), 114.66, 115.42, 117.63, 122.87, 132.11, 132.25 (β-C), 135.53, 143.62 (β-C), 147.88, 148.15, 148.35, 150.19, 158.54. MS: (ESI) m/z 351 (100[M -3Cl] 2+), HRMS: calcd. For C₄₆H₃₃N₁₀: 351.1478 found 351.1481.

Synthesis of **5**: Porphyrin **4** (10.0 mg 0.0141 mmol) was dissolved in water (10 ml) and zinc(II) acetate (3.00 mg, 0.0133 mmol) added. The mixture was stirred at room temperature for 1 hour and checked for completion by TLC. Ammonium hexafluorophosphate was added, and the product filtered. The solid was dissolved in acetone and tetrabutylammonium chloride was added, and the mixture filtered. The crude product was precipitated from diethyl ether over MeOH (10.4 mg, 95 %). UV-vis (H₂O): max, 436, 564, 612. ¹H-NMR (DMSO-d₆): δ 4.72 (s, 9H, CH₃), 7.61 (d, 2H, 5-m-Ph), 8.21 (d, 2H, 5-o-Ph), 8.9-9.06 (m, 14H, 10,15,20-o-Py, βH), 9.44 (m, 6H, 10,15,20-m-Py). ¹³C-NMR (DMSO-d₆): δ 48.26 (CH₂-N₃), 115.26, 116.03, 118.21, 122.73, 132.13, 132.65(β-C), 133.70, 136.13, 139.44, 139.87, 144.22(β-C), 148.75, 148.92, 150.75, 159.10. MS: (ESI) m/z 400 (100[M -2Cl] 2+), HRMS: calcd. For C₄₄H₃₃Cl₁N₁₀Zn₁ : 400.0929 found 400.0932.

Synthesis of **6**: Tetraethylene glycol (2.70 g, 13.9 mmol) was slowly added to a solution of NaH (60 % in mineral oil, 0.8 g, 20 mmol) in THF (20 ml) at -20 °C. Propargyl bromide (80 % in toluene, 1.48 ml, 13.9 mmol) was added after all bubbling stopped and the mixture was stirred overnight at room temperature and nitrogen. The mixture was filtered and solvent removed under

reduced pressure. The crude was then purified by column chromatography (4.5 % MeOH : DCM) to yield the product as a pale yellow oil (1.82 g, 68%). ¹H-NMR (CDCl₃): δ 2.40 (s, 1H, C≡CH), 2.92 (OH), 3.52-3.66 (m, 16H), 4.13 (d, 2H, CH₂-C). ¹³C-NMR- (CDCl₃): δ 58.39 (CH₂-C), 61.68 (CH₂-OH), 69.13, 70.37, 70.41, 70.56, 70.58, 70.65, 72.61, 74.65 (C≡CH), 79.66 (C≡CH). MS: (ESI) m/z 233 (100[M + H]⁺), HRMS: calcd. for C₁₁H₂₁O₅: 233.1384 found 233.1380

Synthesis of **7**: TsCl (1.60 g, 8.39 mmol) and TEA (1.17 ml, 8.39 mmol) were added to a stirred solution of PEG **6** (1.86 g, 8.00 mmol) in DCM. The mixture was stirred under nitrogen at room temperature for 17 hours. The solvent was removed under reduced pressure and the product purified by column chromatography to yield the product as a pale yellow oil (2.47 g, 80 %). ¹H-NMR (CDCl₃): δ 2.38 (s, 4H, C≡CH, CH₃), 3.45-3.65 (m, 14H), 4.02-4.14 (m, 4H, CH₂-C, CH₂), 7.26 (d, 2H, J=7.9 Hz), 7.70 (d, 2H, J=7.1 Hz). ¹³C-NMR (CDCl₃): δ 21.57 (CH₃), 58.41 (CH₂-C), 68.75, 69.09, 69.40, 70.35, 70.54, 70.66, 70.73, 74.76 (C≡CH), 79.73 (C≡CH), 127.98, 129.93, 130.37, 132.95 (4-Ar), 144.92 (1-Ar). MS: (ESI) m/z 404 (100[M + NH₄]⁺), HRMS: calcd. For C₁₈H₃₀O₇N₁S₁ : 404.1737 found 404.1726.

Synthesis of **8**: PEG **7** (2.47 g, 6.40 mmol) was dissolved in 10 ml of anhydrous THF under argon. The solution was heated to 80 °C and a solution of 1 M TBAF in THF (4.84 ml, 4.84 mmol) was added. The product was allowed to cool and the solvent was removed under reduced pressure. The product was purified by column chromatography using (25 % DCM : ethyl acetate) to give a pale yellow oil (1.35 g, 90 %). ¹H-NMR (CDCl₃): δ 2.40 (s, 1H, C-CH), 3.58-3.68(m, 14H), 4.14 (d, 2H, O-CH₂-C), 4.5, 4.8 Hz, 4 Hz(dt, 2H, F-CH₂). ¹³C-NMR (CDCl₃): δ 21.57 (CH₃), 58.40 (CH₂-C), 70.39, 70.59, 70.69, 70.78, 74.62(C≡CH), 79.73 , 82.38, 84.05, 128.97 J = 744 Hz(CH₂-

F). ^{19}F -NMR (CDCl_3): δ 179.50. MS: (ESI) m/z 252 ($100[\text{M} + \text{NH}_4]^+$), HRMS: calcd. For $\text{C}_{11}\text{H}_{23}\text{F}_1\text{O}_4\text{N}_1$: 252.1606 found 252.1607.

Synthesis of **9**: Porphyrin **5** (10.0 mg 0.0118 mmol) was added to a 10 ml microwave tube and PEG **8** (3.00 mg, 0.013 mmol) in THF : water (1 : 3, 8 ml) was added. Copper (II) sulphate pentahydrate (5.00 mg, 0.0200 mmol), sodium ascorbate (5.00 mg, 0.0250 mmol) and TBTA (1.00 mg, 1.90 mmol) were added and the mixture heated to 45 °C by microwave (75 W, max pressure 100 bar) for 20 minutes. The mixture was concentrated under reduced pressure and ammonium hexafluorophosphate was added. The mixture was filtered and redissolved in acetone. Tetrabutylammonium chloride was added and the mixture filtered. The product was precipitated from diethyl ether over MeOH to yield the product as a green solid (11.4 mg, 90 %). UV-vis (H_2O): max, 435, 565, 614 $\log(435 \text{ nm}) = 5.03 \text{ M}^{-1}\text{cm}^{-1}$. ^1H -NMR (DMSO-d_6): δ 3.65 (m, 14H), 4.53, $J=24 \text{ Hz}, 4 \text{ Hz}$ (dt, 2H, $\text{CH}_2\text{-F}$), 4.72 (s, 9H, CH_3), 4.77 (s, 2H, $\text{O-CH}_2\text{-Triazole}$), 8.34-8.44 (m, 4H, 5-Ph), 8.85-9.06 (m, 14H, 10,15,20-m-Py, m 8H, βH), 9.20 (s, 1H, Triazole- H), 9.44 (d, 6H, 10,15,20-o-Py). ^{13}C -NMR (DMSO-d_6): δ 40.13, 48.26, 58.05, 64.06, 69.77, 70.44. MS: (ESI) m/z 333 ($100[\text{M} - 3\text{Cl}]^{3+}$), HRMS: calcd. For $\text{C}_{55}\text{H}_{52} \text{O}_4\text{N}_{10}\text{F}_1\text{Zn}_1$: 333.1144 found 333.1152.

Radiochemistry

Fluorine production: The fluorine-18 radionuclide was produced by the $^{18}\text{O}(\text{p},\text{n})^{18}\text{F}$ reaction on an enriched water target. Oxygen-18 water containing 80 MBq of ^{18}F was transferred to a 5ml V-vial containing potassium carbonate solution in water (0.1M, 200 μl), and Kryptofix K222 (5 μg)

in water (300 μ l). The water was removed via azeotropic distillation with acetonitrile under a compressed air stream at 110 $^{\circ}$ C.

Synthesis of **8**[18 F] via isotopic substitution: To a 5ml V-vial containing the dried 18 F was added **8** (5 mg, 0.021 mmol) in dry DMSO (200 μ l) and the mixture heated to 180 $^{\circ}$ C for 10 minutes. The mixture was diluted with methanol (1 ml) and passed through a Sep-Pak Light Alum N cartridge. Labelling yields were determined by radioTLC, and the mixture was used without further purification.

Synthesis of **8**[18 F] from **7**: To a 5ml V-vial containing the dried 18 F was added **7** (5 mg, 0.013 mmol) in dry DMSO (200 μ l) and the mixture heated to 140 $^{\circ}$ C for 10 minutes. The mixture was diluted with methanol (1 ml) and passed through a Sep-Pak Light Alum N cartridge. Labelling yields were determined by radioTLC, and the mixture was used without further purification.

Synthesis of carrier-added **8**[18 F]: To a 5ml V-vial containing the dried 18 F was added **7** (5 mg, 0.013 mmol) in dry DMSO (200 μ l) and the mixture heated to 140 $^{\circ}$ C for 10 minutes. Tetrabutylammonium fluoride (5 mg, 0.019 mmol) in dry DMSO (200 μ l) was added and the mixture heated to 140 $^{\circ}$ C for 5 minutes. The mixture was diluted with methanol (1.5 ml) and purified on a Sep-Pak Light Alum N cartridge. Labelling yields were determined by radio-TLC, and the mixture was used without further purification.

General methodology for click reaction **9**[18 F]: To a 10 ml microwave tube containing **8**[18 F] was added **5** (1 mg, 1.1 μ mol) in water (0.2 ml) and a solution of TBTA (174 μ g, 0.4 μ mol), and

copper (II) sulfate pentahydrate (50 μg , 0.2 μmol) and sodium ascorbate (80 μg , 0.4 μmol) in water (0.2 ml). The mixture was heated to 40 $^{\circ}\text{C}$ for 20 minutes (MW, 60 W). The mixture was diluted with water (20 ml) and passed through a Sep-Pak Light C18 cartridge. The cartridge was washed with water (5 ml) and the product eluted with ethanol (0.5 ml).

***in vivo* Radiochemistry**

Fluorine production: Oxygen-18 water (~140 μL) containing 1.8 GBq of ^{18}F was transferred to a 5 ml V-vial containing potassium hydrogencarbonate solution (0.5 ml, 5 mg/ml) and Kryptofix K222 (10.2 mg in 1 ml of dry acetonitrile). The water was removed via azeotropic distillation with acetonitrile under a compressed argon stream at 90 $^{\circ}\text{C}$.

Synthesis of **8**[^{18}F]: To a 5 ml V-vial containing dried 18F (1.4 GBq) was added **7** (6.7 mg) in dry acetonitrile (1 ml) and the mixture heated to 90 $^{\circ}\text{C}$ for 10 minutes. The crude reaction mixture was passed through Sep-Pak Light Alum N cartridge. Eluted activity: 982 MBq, (RCY 77%.) The solvent was reduced to ~ 0.2 ml at 90 $^{\circ}\text{C}$ under a compressed argon stream and the residue diluted with water (0.5 ml). The crude was purified on semi-preparative HPLC (MeCN:water, 20% to 30% in 15 min), with **8**[^{18}F] eluting at 10-11 min (726 MBq). The collected HPLC fraction was diluted to 40 ml with water and loaded on home-made Oasis C18 Lite Sep-Pak cartridge, washed with water (10 ml) and eluted with methanol (2 ml). Methanol solution containing activity was dried at 60 $^{\circ}\text{C}$.

Synthesis of **9**[^{18}F]: To a 1.7 ml champagne HPLC vial containing pure **8**[^{18}F] (446 MBq) was added a combined solution of copper (II) sulfate pentahydrate (0.5 mg in 12.5 μl water), sodium ascorbate (3.75 mg in 50 μl water), TBTA (0.5 mg in 160 μl methanol) and porphyrin (0.2 mg in 100 μl water). The reaction mixture was heated to 60 $^{\circ}\text{C}$ for 35 minutes. The crude product was

purified on semi-preparative HPLC (MeCN:water, 20% to 40% in 30 min) with **9**[¹⁸F] eluting at 15-16 min (72.6 MBq, RCY 16.2 %). The fraction was diluted with water and purified on an Oasis C18 Sep-Pak cartridge. The product was eluted with ethanol (0.5 ml) while filtering on a 0.22 µm filter. The solution was evaporated to dryness under stream of compressed argon at 60°C and dissolved in 0.2 uL of heparin-water (33.6 MBq).

Quality control

All reactions were monitored, and incorporation was determined by radio-TLC using silica TLC sheets, in 9:1 DCM/MeOH solution. RCY and RCP was determined for all compounds using analytical HPLC under gradient conditions (MeCN:water with 0.1 % TFA, 25-40 % over 30 mins). The compounds were eluted after the following retention times (tR): **8**[¹⁸F] 8.5 min, **9**[¹⁸F] 16:6 min.

Partition coefficient determination

9[¹⁸F] (3.4 MBq) was partitioned in a mixture of 1 ml of 1-octanol and 1 ml of PBS after being vortexed for 5 min. Following centrifugation at >1,200 g for 5 min, the octanol and aqueous phases were sampled and counted. Reported log P value is based on the average of three samples.

PET imaging

CD-1 nu/nu female mice (Charles River, UK) bearing subcutaneous HT29 or U87 xenografts of 200-600mm³ were anaesthetised with 1–2% Isoflurane, the tail vein was catheterised and they were placed in the Minerve Small-Animal Imaging Cell (Minerve, France) and transferred to the SuperArgus 2R preclinical PET/CT scanner (Sedecal, Spain). At the start of the PET acquisition,

animals were injected with ~10MBq of ^{18}F -9 intravenously (IV) via the tail vein and 90-minutes of data were acquired using the 250-700 keV energy window. Data was histogrammed into 3 x 120, 1 x 240, 4 x 600 and 2 x 1200-second bins and reconstructed into a 175 x 175 x 61 (0.3875 x 0.3875 x 0.775mm) matrix using OSEM2D with 16 subsets and 2 iterations and randoms/scatter/attenuation correction via Sedecal MMWKS software. The image data was normalized to correct for nonuniformity of response, dead-time count losses and radioactive decay to the time of injection. Activity concentrations were determined by conversion of count rate data from reconstructed images. Regions of interest were drawn around the tumour and sections of quadriceps muscle and liver, and time-activity curves generated using AMIDE software²⁹ (Loening & Gambhir, Molecular Imaging 2003). CT images were acquired via 360 projections/8 shots at a tube voltage of 45kV and current of 140 μ A. Respiration and temperature were monitored throughout using the SA Instruments 1025T monitoring system (SA Instruments, CA, USA). All procedures were carried out in accordance with the Animals in Scientific Procedures Act 1986 and UKCCCR Guidelines 2010 by approved protocols following institutional guidelines (Home Office Project License number 60/4549 held by Dr. Cawthorne).

Author Information

Corresponding Author

*E-mail R.W.Boyle@hull.ac.uk. Phone: +44 [1482466353]

Author Contributions

The manuscript was written with contributions from all authors, with approval upon final version.

Conflict of interest

The authors declare no competing financial interest.

Acknowledgements

We are grateful to Gonçalo Clemente for production of fluorine-18. Mass spectrometry data was acquired at the EPSRC UK National Mass Spectrometry Facility at Swansea University.

Supporting Information

Video of overall biodistribution over time in mouse model.

References

- (1) Kelkar, S. S.; Reineke, T. M. Theranostics: Combining Imaging and Therapy. *Bioconjugate Chem.* **2011**, *22* (10), 1879–1903.
- (2) Josefsen, L. B.; Boyle, R. W. Unique Diagnostic and Therapeutic Roles of Porphyrins and Phthalocyanines in Photodynamic Therapy, Imaging and Theranostics. *Theranostics* **2012**, *2* (9), 916–966.
- (3) Zheng, H. A Review of Progress in Clinical Photodynamic Therapy. *Technol. Cancer Res. Treat.* **2005**, *4* (3), 283–293.
- (4) O'Connor, A. E.; Gallagher, W. M.; Byrne, A. T. Porphyrin and Nonporphyrin Photosensitizers in Oncology: Preclinical and Clinical Advances in Photodynamic Therapy. *Photochem. Photobiol.* **2009**, *85* (5), 1053–1074.
- (5) Ethirajan, M.; Chen, Y.; Joshi, P.; Pandey, R. K. The Role of Porphyrin Chemistry in Tumor Imaging and Photodynamic Therapy. *Chem. Soc. Rev.* **2011**, *40* (1), 340–362.
- (6) Phelps, M. PET Molecular Imaging and Its Biological Applications, 1st ed.; Phelps, M., Ed.; Springer: New York, 2004; pp 200-202
- (7) Shi, J.; Liu, T. W. B.; Chen, J.; Green, D.; Jaffray, D.; Wilson, B. C.; Wang, F.; Zheng, G. Transforming a Targeted Porphyrin Theranostic Agent into a PET Imaging Probe for Cancer. *Theranostics* **2011**, *1*, 363–370.

- (8) Ranyuk, E. R.; Cauchon, N.; Ali, H.; Lecomte, R.; Guérin, B.; van Lier, J. E. PET Imaging Using ^{64}Cu -Labeled Sulfophthalocyanines: Synthesis and Biodistribution. *Bioorg. Med. Chem. Lett.* **2011**, *21* (24), 7470–7473.
- (9) Mukai, H.; Wada, Y.; Watanabe, Y. The Synthesis of ^{64}Cu -Chelated Porphyrin Photosensitizers and Their Tumor-Targeting Peptide Conjugates for the Evaluation of Target Cell Uptake and PET Image-Based Pharmacokinetics of Targeted Photodynamic Therapy Agents. *Ann. Nucl. Med.* **2013**, *27* (7), 625–639.
- (10) Zoller, F.; Riss, P. J.; Montforts, F.-P.; Kelleher, D. K.; Eppard, E.; Rösch, F. Radiolabelling and Preliminary Evaluation of ^{68}Ga -Tetrapyrrole Derivatives as Potential Tracers for PET. *Nucl. Med. Biol.* **2013**, *40* (2), 280–288.
- (11) Azad, B. B.; Cho, C.; Lewis, J. D.; Luyt, L. G. Synthesis, Radiometal Labeling and in Vitro Evaluation of a Targeted PPIX Derivative. *Appl. Radiat. Isot.* **2012**, *70* (3), 505–511.
- (12) Vahidfar, N.; Jalilian, A. R.; Fazaeli, Y.; Bahrami-Samani, A.; Beiki, D.; Khalaj, A. Development and Evaluation of a $^{166}\text{holmium}$ Labelled Porphyrin Complex as a Possible Therapeutic Agent. *J. Radioanal. Nucl. Chem.* **2012**, *295* (2), 979–986.
- (13) Waghorn, P. A. Radiolabelled Porphyrins in Nuclear Medicine. *J. Labelled Compd. Radiopharm.* **2013**, *57* (4), 1–10.

- (14) Kavali, R.; Lee, B. C.; Moon, B. S.; Yang, S. D.; Chun, K. S.; Choi, C. W.; Lee, C. H.; Chi, D. Y. Efficient Methods for the Synthesis of 5-(4-[¹⁸F]fluorophenyl)-10,15,20-tris(3-Methoxyphenyl)porphyrin as a Potential Imaging Agent for Tumor. *J. Labelled Compd. Radiopharm.* **2005**, (10), 749–758.
- (15) Ranyuk, E.; Ali, H.; Guerin, B.; Van Lier, J. A New Approach for the Synthesis of ¹⁸F-Radiolabelled Phthalocyanines and Porphyrins as Potential Bimodal/Theranostic Agents. *J. Porphyrins Phthalocyanines.* **2013**, 17 (8/9), 850–856.
- (16) Bryden, F.; Boyle, R. W. A Mild, Facile, One-Pot Synthesis of Zinc-Azido Porphyrins as Substrates for Use in Click Chemistry. *Synlett* **2013**, 24, 1978-1982.
- (17) Giuntini, F.; Bryden, F.; Daly, R.; Scanlan, E. M.; Boyle, R. W. Huisgen-Based Conjugation of Water-Soluble Porphyrins to Deprotected Sugars: Towards Mild Strategies for the Labelling of Glycans. *Org. Biomol. Chem.* **2014**, 12 (8), 1203–1206.
- (18) Giuntini, F.; Dumoulin, F.; Daly, R.; Ahsen, V.; Scanlan, E. M.; Lavado, A. S. P.; Aylott, J. W.; Rosser, G. A.; Beeby, A.; Boyle, R. W. Orthogonally Bifunctionalised Polyacrylamide Nanoparticles: A Support for the Assembly of Multifunctional Nanodevices. *Nanoscale* **2012**, 4 (6), 2034–2045.
- (19) Rostovtsev, V. V.; Green, L. G.; Fokin, V. V.; Sharpless, K. B. A Stepwise Huisgen Cycloaddition Process: Copper(I)-Catalyzed Regioselective “Ligation” of Azides and Terminal Alkynes. *Angew. Chem., Int. Ed. Engl.* **2002**, 41 (14), 2596–2599.

- (20) Boyle, R. W.; Clarke, O. J.; Sutton, J. M.; Greenman, J. Chromophores. US Patent 0203888 A1, October 30, 2003.
- (21) Sutton, J. M.; Clarke, O. J.; Fernandez, N.; Boyle, R. W. Porphyrin, Chlorin, and Bacteriochlorin Isothiocyanates: Useful Reagents for the Synthesis of Photoactive Bioconjugates. *Bioconjugate Chem.* **2002**, *13* (2), 249–263.
- (22) Bryden, F.; Maruani, A.; Savoie, H.; Chudasama, V.; Smith, M. E. B.; Caddick, S.; Boyle, R. W. Regioselective and Stoichiometrically Controlled Conjugation of Photodynamic Sensitizers to a HER2 Targeting Antibody Fragment. *Bioconjugate Chem.* **2014**, *25* (3), 611–617.
- (23) Goswami, L. N.; Houston, Z. H.; Sarma, S. J.; Jalisatgi, S. S.; Hawthorne, M. F. Efficient Synthesis of Diverse Heterobifunctionalized Clickable Oligo(Ethylene Glycol) Linkers: Potential Applications in Bioconjugation and Targeted Drug Delivery. *Org. Biomol. Chem.* **2013**, *11* (7), 1116–1126.
- (24) Harris, J. M.; Struck, E. C.; Case, M. G.; Paley, S.; Yalpani, M. Synthesis and Characterisation of Poly(Ethylene Glycol) Derivatives. *J. Polym. Sci.* **1984**, *22* (2), 341–352.
- (25) Schwach, G.; Thamyongkit, P.; Reith, L. M.; Svejda, B.; Knör, G.; Pfragner, R.; Schoefberger, W. A Water Soluble Tri-Cationic Porphyrin-EDTA Conjugate Induces Apoptosis in Human Neuroendocrine Tumor Cell Lines. *Bioorg. Chem.* **2012**, *40* (1), 108–113.

- (26) Prabhakar, U.; Maeda, H.; Jain, R. K.; Sevick-Muraca, E. M.; Zamboni, W.; Farokhzad, O. C.; Barry, S. T.; Gabizon, A.; Grodzinski, P.; Blakey, D. C. Challenges and Key Considerations of the Enhanced Permeability and Retention Effect for Nanomedicine Drug Delivery in Oncology. *Cancer Res.* **2013**, *73* (8), 2412–2417.
- (27) Huang, S.; Shao, K.; Liu, Y.; Kuang, Y.; Li, J.; An, S.; Guo, Y.; Ma, H.; Jiang, C. Tumor-Targeting and Microenvironment-Responsive Smart Nanoparticles for Combination Therapy of Antiangiogenesis and Apoptosis. *ACS Nano.* **2013**, *7* (3), 2860–2871.
- (28) Hollis, C. P.; Weiss, H. L.; Leggas, M.; Evers, B. M.; Gemeinhart, R. A.; Li, T. Biodistribution and Bioimaging Studies of Hybrid Paclitaxel Nanocrystals: Lessons Learned of the EPR Effect and Image-Guided Drug Delivery. *J. Control. Release.* **2013**, *172* (1), 12–21.
- (29) Loening, A. M.; Gambhir, S. S. AMIDE: A Free Software Tool for Multimodality Medical Image Analysis. *Mol. Imaging.* **2003**, *2* (3), 131-137.